PERIODIC OUTPUT FEEDBACK CONTROL FOR HELICOPTER VIBRATION REDUCTION

Claudio Brillante[*], **Marco Morandini**[†], **Paolo Mantegazza**[‡]

Dipartimento di Scienze e Tecnologie Aerospaziali,
Politecnico di Milano, Italy
[*]claudio.brillante@mail.polimi.it,
[†]marco.morandini@polimi.it,
[‡]paolo.mantegazza@polimi.it

Keywords: Periodic control, output feedback, active twist blade, individual blade control.

Abstract: This paper investigates the potentiality of the periodic direct output feedback (POF) control to reduce rotor vibrations in forward flight. The blade control strategy relies on their active twist actuation. The blades are twisted by means of macro-fiber composite (MFC) piezoelectric actuators distributed along the span. The multibody software MBDyn is used to model the isolated rotor of the Bo105, with the original blades replaced by actively controlled ones. The periodic output feedback controller reduces the hub loads by minimizing selected harmonics of the blade root shear force. The results are compared with those obtained with a periodic H_2 optimal controller. All the closed loop analysis are performed by simulating the rotor dynamics with MBDyn while running the control code in Simulink. A specialized communication library is used to coordinate the co-simulation and exchange data between the two codes.

NOMENCLATURE

c	Blade choord
F_z	Blade root shear force
F_Z	Hub vertical force
M_X	Hub moment along x axis
M_Y	Hub moment along y axis
T_Z	Rotor thrust
p	Pitch bearing position
R	Blade radius
V	Electric potential
V_∞	Free stream velocity
α	Shaft angle
ϑ_p	Precone angle
ϑ_{tw}	Blade twist

μ	Advancing parameter
ν_β	Non-dimensional flap frequency
ν_ϑ	Non-dimensional torsional frequency
ν_ξ	Non-dimensional lag frequency
Ω	Rotor angular velocity
$E\{.,.\}$	Variance matrix

INTRODUCTION

Helicopter vibration and internal noise reduction is being actively pursued by helicopter makers. Active controls can play an important role, and one of the proposed strategies pursued so far to alleviate hub loads is to modify the periodic aerodynamic loads at harmonic frequencies above the 1/rev. The classical higher harmonic control (HHC) [1] is based on a linear quasi-static rotor response and computes a suitable, vibration cancelling high harmonic signal for the swashplate. The HHC approach has been widely used. However, the availability of technologies allowing to embed the actuators into the blades permits the so called individual blade control (IBC), in which each blade is controlled independently [2, 3, 4, 5]. This paper assumes the availability of actively twisted blades, with the active twist induced by piezoelectric actuators distributed along the blade span. The control voltage is computed to minimize the aerodynamic loads. Many works do exist in the literature about active twist rotors (ATRs). Furthermore, experimental tests carried out at NASA [2]and DLR [6, 7] proved the technological feasibility of such a solution. Other interesting applications of ATRs can be found in [8] and in [9].

Since the rotor subsystem exhibits a nonlinear behavior in both the structural dynamics of the blades and the aerodynamic field, linear time invariant control theory often fails to provide satisfactory results. A more sophisticate solution is to design a periodic controller, thus taking into account the periodicity of the rotor in forward flight. An implementation of the model following approach to stabilize the lag and pitch moments using periodic control can be found in [10]. Applications of periodic control in the reduction of vibrations by means of IBC are reported in [11, 12], where the alleviation of the baseline loads is considered as a disturbance rejection problem. In [13] a more sophisticated periodic controller based on the H_2 and H_∞ design is exploited to reduce hub loads through active trailing edge flaps.

The current work is basically an extension of a previous study on periodic control applied on ATRs [14]. Here the periodic static output feedback control theory is investigated because its design involves fewer parameters than those of an H_2 dynamic compensator. This paper aims at showing that satisfactory results can be achieved even using the static controller approach, which is also the easiest solution with a view of a scheduling approach. The work is organized as follows. First, the rotor numerical model is briefly described. Then, the blade response is properly identified and a periodic direct output feedback controller is designed. The closed loop simulation results are then shown and compared with those obtained with the H_2 optimal solution.

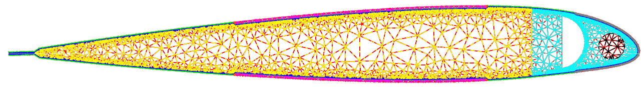

Figure 1: Blade section discretization.

Table 1: BO 105 model data with original and piezoelectric blade.

Rotor data	BO 105 blade	Piezoelectric blade
R	4.9 m	4.9 m
p	0.23 m	0.23 m
ϑ_p	$2.5°$	$2.5°$
c	0.3025 m	0.3025 m
ϑ_{tw}	$-8°$	$-8°$
Ω	44.4 rad/s	44.4 rad/s
α	$3°$	$3°$
ν_β	1.11	1.1
ν_ξ	0.69	0.73
ν_ϑ	3.63	3.89

NUMERICAL ROTOR MODEL

The test bed of this work is an available numerical model of the Bo105 rotor[15]. We focus our attention only on the main rotor subsystem. The kinematics and the flexbeams characteristics of the main original rotor are left unchanged. The blades, instead, are replaced with actively twisted ones, embedding piezoelectric actuators distributed along the blade span. Macro-fiber composite (MFC) actuators with interdigitated electrodes are used, since they exploit the primary piezoelectric direction of polarization and thus allow a high strain rate with low actuation power. In order to generate the highest possible torsional control on the blades, they are oriented in such a way that the strain is applied at $\pm 45°$.

The available rotor data are employed to build a deformable multibody model through the multibody code MBDyn [16]. The swashplate and the pitch links are represented with rigid bodies, while each blade is modeled using five geometrically exact finite volume nonlinear beam elements [17]. The software can handle piezoelectrically actuated beams provided the stiffness and the piezoelectric coupling matrix of the blade section are known. While the data of the original Bo105 blades are known, the section properties of the actively twisted blades are computed by employing the semi-analytical approach described in [18, 19, 20], which takes into account three dimensional effects. Within this approach the three dimensional continuum is decomposed into the one dimensional domain of the beam model and the two dimensional domain of the beam section, which is solved by a specialized finite element based analysis, as shown in fig. 1. The designed piezoelectric blade has to satisfy constraints about the position of the elastic axis and the center of mass so to avoid aeroelastic instabilities; therefore, the optimization procedure described in [21] is used to impose these constraints while maximizing the actuation power. Rotor data and the set of lowest frequencies accounted for the original and the piezoelectric blade are shown in tab. 1.

The multibody software MBDyn implements simple aerodynamic theories for the isolated helicopter rotor analysis. These models, although very simple, permit fast simulations with a level of accuracy adequate to reproduce representative vibratory loads in forward flight within a preliminary design of the controller. The chosen aerodynamic model is based on the blade element theory combined with the Drees inflow model. The Bo105 blades are built using the shape of the NACA 23012 airfoil. The software requires as input a data sheet with information about the variation of the lift and drag coefficients, C_L and C_D, with respect to the Mach number and the aerodynamic angle of attach.

PERIODIC OUTPUT FEEDBACK VIBRATION CONTROL

System identification

Since the aerodynamic theory is very simple, there is no interference among the actuation of one blade and the forces on other blades. Thus, each blade can be controlled independently. Therefore, only an isolated blade is considered in the controller design. The periodic control theory requires a state space model of the blade response, which will be properly identified in this section . What we are interested in is a linearized model of the blade mapping the applied voltage on the blade V to the measured variables on the blade. To such an end it has been decided to take into account the vertical force acting on the blade root, F_Z, and 5 vertical accelerations uniformly distributed along the blade span, with the baseline loads subtracted so to have a linearized model around an equilibrium solution. Before the identification, each measure has been suitably filtered so that the signals include only the 3/rev and the 4/rev harmonics, i.e. those to be minimized. A periodic subspace identification algorithm [22] has been used to find the equivalent linear discrete-time periodic (LTP) model of the blade

$$\begin{aligned} \mathbf{x}_{k+1} &= \mathbf{A}_k \mathbf{x}_k + \mathbf{B}_k u_k \\ \mathbf{y}_k &= \mathbf{C}_k \mathbf{x}_k \end{aligned} \tag{1}$$

where the system matrices have period N.

The input/output time histories signals from the numerical simulations are organized in input/output Hankel matrices $\mathbf{U}_{k,s}$ and $\mathbf{Y}_{k,s}$ for $k = 1 \dots N$ as follows

$$\mathbf{U}_{k,s} = \begin{bmatrix} u_k & u_{k+1} & \cdots & u_{k+s-1} \\ u_{N+k} & u_{N+k+1} & \cdots & \vdots \\ \vdots & & \cdots & \vdots \\ u_{(n-1)N+k} & & \cdots & u_{(n-1)N+k+s-1} \end{bmatrix} \tag{2}$$

$$\mathbf{Y}_{k,s} = \begin{bmatrix} y_k & y_{k+1} & \cdots & y_{k+s-1} \\ y_{N+k} & y_{N+k+1} & \cdots & \vdots \\ \vdots & & \cdots & \vdots \\ y_{(n-1)N+k} & & \cdots & y_{(n-1)N+k+s-1} \end{bmatrix}, \tag{3}$$

where N is the period, n is the total number of simulations and s is the duration of each experiment. The Hankel matrices are here computed using the results of just one numerical simulation. Considering the QR factorization of the compound matrices

$$\begin{bmatrix} \mathbf{U}_{k,s} & \mathbf{Y}_{k,s} \end{bmatrix} = \begin{bmatrix} \mathbf{Q}_{1_k} & \mathbf{Q}_{2_k} \end{bmatrix} \begin{bmatrix} \mathbf{R}_{11_k} & \mathbf{R}_{12_k} \\ \mathbf{R}_{21_k} & \mathbf{R}_{22_k} \end{bmatrix}, \tag{4}$$

the observability matrix $\mathbf{O}_k$ is given by the row space of matrix $\mathbf{R}_{22_k}$. It can be computed through its singular value decomposition (SVD)

$$\mathbf{R}_{22_k} = \mathbf{U}_k \Sigma_k \mathbf{V}_k^T, \tag{5}$$

$$\mathbf{O}_k = \tilde{\mathbf{V}}_k^T. \tag{6}$$

The matrix $\tilde{\mathbf{V}}_k^T$ contains the first rows and columns of $\mathbf{V}_k^T$ based on the chosen order of the identified system, which depends on the magnitude of the singular values. The matrices $\mathbf{A}_k$ and $\mathbf{C}_k$ can then be obtained by exploiting the observability matrix at the instants $k+1$ and k as described in [22, 13]. The periodicity is imposed by setting $\mathbf{O}_{N+1} = \mathbf{O}_1$.

Matrices $\mathbf{B}_k$ and $\mathbf{D}_k$ are computed through an output error approach by minimizing the squared 2-norm error between the real and the model output, y_{real} and y respectively:

$$\min_{\mathbf{B}_k, \mathbf{D}_k} \parallel y_{real} - y \parallel_2^2 . \tag{7}$$

Two simulations have to be carried out before starting the identification procedure. This is because the identified blade model is a linearization of the blade response around the trim condition. The first simulation is required to compute the baseline loads, to be subtracted from the output of the second simulation, in which the blade is randomly excited. The voltage random signal has an amplitude of 40 V and is suitably filtered above the 6/rev so to limit higher harmonics in the dynamic response. The aeroelastic multibody simulation requires a small time step to avoid numerical problems and in this article $N = 140$ time steps per rotor revolution are used. These time steps will lead to an identification of 140 linear systems spanning the period. This computational burden can be reduced because the output of the simulation can be well approximated with a larger time step. Therefore, the output is decimated to $N = 28$ time steps per rotor revolution. Having defined a larger time step for the LTP model of the blade, the output of the multibody simulations are resampled and an identification technique based on a subspace algorithm is adopted. Hints about the order of the identified system can be found by analyzing the singular value magnitudes of the matrix $\mathbf{R}_{22_k}$ at each time step. Figure 2 shows the singular values for the first time step of the period and the best compromise between data fitting and system order is given by retaining the most important singular values. In this work the linear periodic model of the blade is a $14th$ order system for every time step spanning the period.

Controller design

The goal of this section is to develop a periodic static output feedback controller to reduce rotor vibrations through individual blade control. In the general case the sought output feedback control law is given by

$$u_k = \mathbf{K}_k \mathbf{y}_k, \tag{8}$$

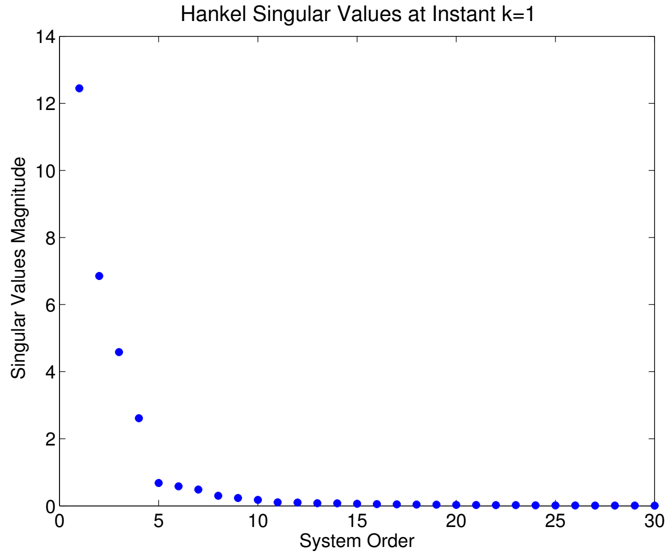

Figure 2: System order.

where the gain matrix $\mathbf{K}_k$ can be periodic with period N or simply a constant matrix equal throughout the period. Thanks to the periodicity of the system, a single controller is designed for a single blade. If the time variable approach is used, the same controller can be used for all the remaining blades after applying a time shift to the gain matrix.

In the present work we want to minimize appropriate harmonics of the blade root loads, and the baseline load condition has to be considered in the design model. They are introduced as a disturbance to the plant output as shown in the block diagram of fig. 3 where z is the controlled output, $\mathbf{y}$ are the measures, $\mathbf{w}$ are white noise disturbances and u the applied blade voltage. The generalized plant model is then described with the following linear periodic model

$$\begin{aligned} \mathbf{x}_{k+1} &= \mathbf{A}_k \mathbf{x}_k + \mathbf{B}_{1_k} \mathbf{w}_k + \mathbf{B}_{2_k} u_k, \\ z_k &= \mathbf{C}_{1_k} \mathbf{x}_k + \mathbf{D}_{11_k} \mathbf{w}_k + \mathbf{D}_{12_k} u_k, \\ \mathbf{y}_k &= \mathbf{C}_{2_k} \mathbf{x}_k + \mathbf{D}_{21_k} \mathbf{w}_k. \end{aligned} \tag{9}$$

The output feedback control law is obtained by minimizing the quadratic performance index

$$J = E\left\{ \sum_{k=0}^{\infty} \left[z_k^T Q_k z_k + u_k^T R_k u_k \right] \right\}, \tag{10}$$

where Q_k and R_k are symmetric periodic user-defined weights. In general no closed form solutions can be found to this problem, and its solution is found through numerical optimization. The problem can be reformulated as explained in [23]. Since the most common optimization algorithms require the gradient of the cost function, it can be computed as

$$J(\mathscr{K}) = tr(\sigma \mathscr{P} \mathscr{G}) \tag{11}$$

$$\nabla_{\mathscr{K}} J(\mathscr{K}) = 2(\mathscr{R} \mathscr{K} \mathscr{C}_2 + \mathscr{B}_2^T \sigma \mathscr{P} \overline{\mathscr{A}}) \mathscr{S} \mathscr{C}_2^T \tag{12}$$

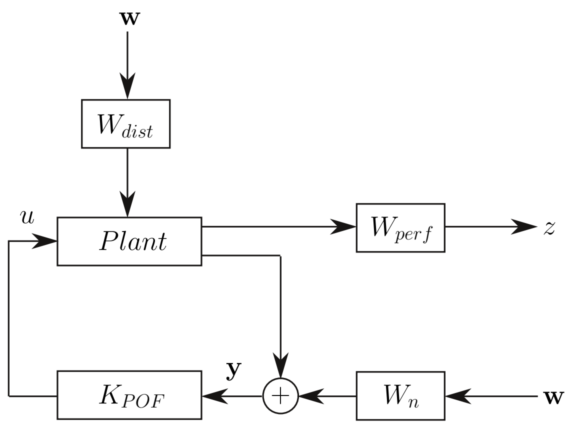

Figure 3: Generalized plant.

The script notation $\mathscr{X}$ indicates the block diagonal matrix $\mathscr{X} = diag(\mathbf{X}_1, \dots, \mathbf{X}_N)$ related to the cyclic sequence of the periodic matrix $\mathbf{X}_k$ and we denote with $\sigma\mathscr{X}$ the K-cyclic shift $\sigma\mathscr{X} = diag(\mathbf{X}_2, \dots, \mathbf{X}_N, \mathbf{X}_1)$. Matrices $\mathscr{P}$ and $\mathscr{S}$ satisfy the discrete periodic Lyapounov equations (DPLEs)

$$\mathscr{P} = \overline{\mathscr{A}}^T \sigma\mathscr{P}\overline{\mathscr{A}} + \overline{\mathscr{Q}} \tag{13}$$

and

$$\sigma\mathscr{S} = \overline{\mathscr{A}}\mathscr{S}\overline{\mathscr{A}}^T + \mathscr{G}, \tag{14}$$

respectively, where $\overline{\mathscr{A}} = \mathscr{A} + \mathscr{B}_2\mathscr{K}\mathscr{C}_2$ is the closed loop matrix and $\overline{\mathscr{Q}} = \mathscr{Q} + \mathscr{C}_2^T\mathscr{K}^T\mathscr{R}\mathscr{K}\mathscr{C}_2$. For the solution of the DPLEs the reader is referred to the Appendix. The matrix $\mathscr{G}$ is defined as $\mathscr{G} = diag(0, \dots, 0, \mathbf{X}_0)$. Supposing that there is no cross-correlation between the initial conditions $\mathbf{x}_0$ and the disturbances $\mathbf{w}$, i.e. $E\left\{\mathbf{x}_0\mathbf{w}^T\right\} = 0$, the matrix $\mathbf{X}_0$ is given by $\mathbf{X}_0 = E\left\{\mathbf{x}_0\mathbf{x}_0^T\right\} + \mathbf{B}_{1_N}E\left\{\mathbf{w}\mathbf{w}^T\right\}\mathbf{B}_{1_N}^T + \mathbf{B}_{2_N}\mathbf{K}_N\mathbf{D}_{21_N}E\left\{\mathbf{w}\mathbf{w}^T\right\}\mathbf{B}_{1_N}^T + \mathbf{B}_{1_N}E\left\{\mathbf{w}\mathbf{w}^T\right\}\mathbf{D}_{21_N}^T\mathbf{K}_N^T\mathbf{B}_{2_N}^T +$ $\mathbf{B}_{2_N}\mathbf{K}_N\mathbf{D}_{21_N}E\left\{\mathbf{w}\mathbf{w}^T\right\}\mathbf{D}_{21_N}^T\mathbf{K}_N^T\mathbf{B}_{2_N}^T$ (the variance matrices are here approximated as identity matrices). Further explanations and details about the output feedback controller design can be found in [24].

The baseline loads and the sensors noise are considered in the generalized plant assembly as output disturbances by the shaping filters W_{dist} and W_n respectively. Figure 4a shows for simplicity only the baseline load of the blade tip acceleration; since the measures have been previously filtered, only the $3/\text{rev}$ and the $4/\text{rev}$ harmonics of the baseline signals have to be reproduced. The sensors noise is represented with constant gains having a value of 0.1. The performance of the controller are defined by means of the frequency weighting function W_{perf} shown in the block diagram of fig. 3. The system output, that we want to reduce is the blade root shear force F_Z and the adopted performance specification W_{perf} is shown in fig. 4b. Dealing with a 4 blade rotor, the reduction of the $4/\text{rev}$ harmonic of the shear blade forces will lead to a decrease of the vertical hub load. W_{perf} prescribes the minimization of $3/\text{rev}$ harmonic as well in order to reduce vibratory loads associated to the bending moment of the blade root load, that will lead to a reduction of the in-plane hub loads. Since all specifications of the desired output are taken into account in the frequency domain by W_{perf}, the performance weight Q_k of the cost function J is set to 1 and is kept constant for the

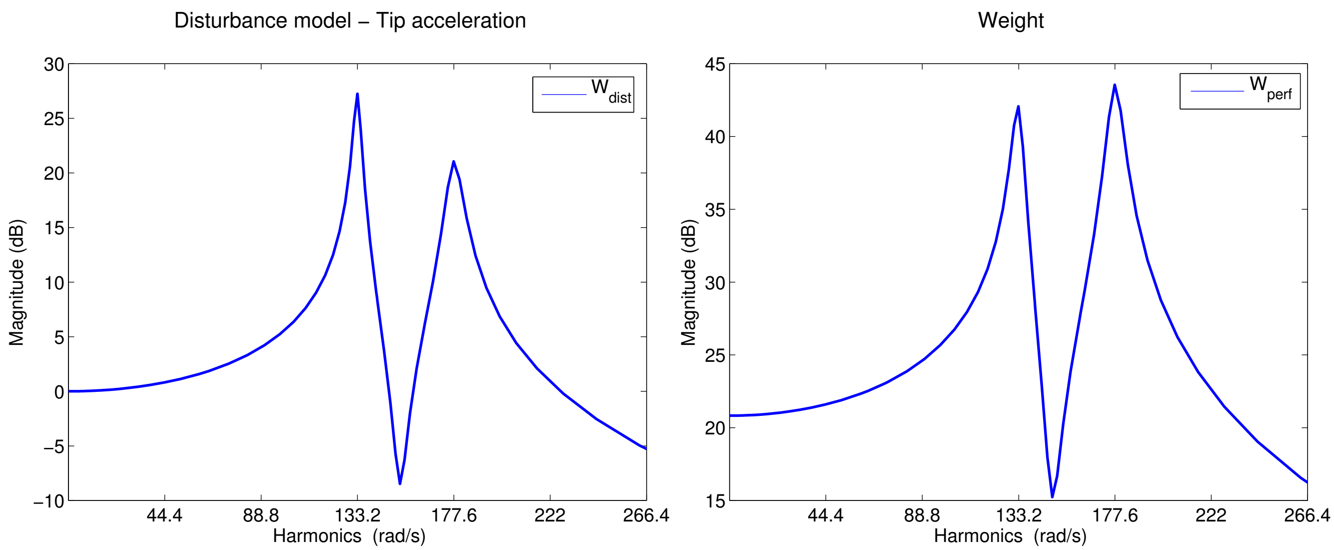

(a) Baseline tip acceleration.

(b) Performance specification.

Figure 4: Generalized plant weights.

whole period, while the other weight R_k, which prescribes a constraint for the control signal, is tuned untill the controller achieves satisfactory results and at the end of the tuning process it has a value of 5000. With the performance criteria defined above, the resulting generalized plant of eq. 9 is a $44th$ order system. In this work we chose a constant gain $(1x6)$ matrix $\mathbf{K}$, and only six parameters have to be computed through the optimization algorithm, which is consequently very fast with respect to the design of the full information H_2 periodic controller. This is also due to fact that the DPLEs can be solved very efficiently in contrast with the solution of the discrete time periodic Riccati equations [25]. The design model is already stable, therefore there is no need to search for a suitable initial solution, which is hence assumed as the null matrix.

SIMULATION RESULTS

The performance of the periodic controller are tested on a trim configuration at $\mu = 0.23$. The rotor is trimmed in order to reproduce reasonable thrust, $T_Z = 20010$ N, and moments, $M_X = 746$ Nm and $M_Y = -85$ Nm, with a shaft angle of $\alpha = 3°$ as in fig. 5.

The swashplate orientation is set in order to achieve the desired trim configuration. The closed loop simulation is carried out by coupling MBDyn with Simulink. The communication between the two programs is managed by bidirectional sockets which allows to exchange data between the two codes. The closed loop simulation can be entirely performed in the Simulink environment, in which the multibody model of the rotor appears as Simulink blocks. Since the multibody simulation and the controller have been designed using different sample times, Simulink Rate-Transition blocks are used to implement a sample and hold procedure, thus overcoming this issue.

To better evaluate the effect of using a static controller, such as that developed here, the direct output feedback controller results has to be compared with those of the optimal solution achieved

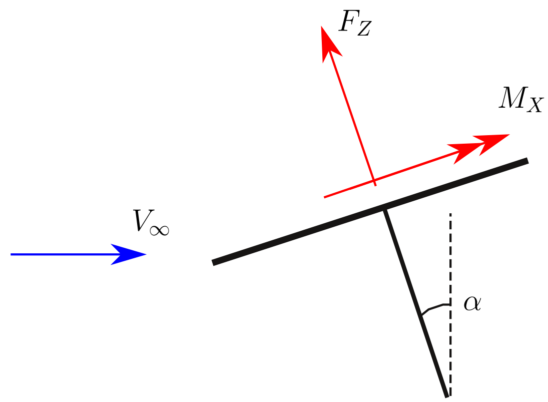

Figure 5: Inclination of rotor shaft.

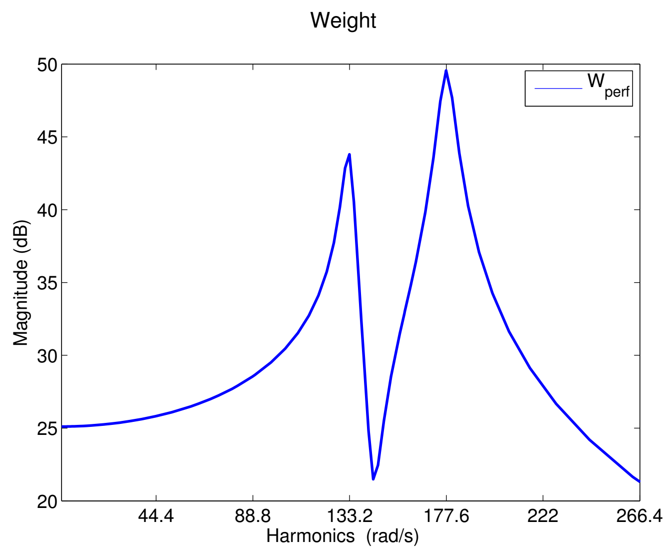

Figure 6: H2 Control performance weight.

by implementing a dynamic compensator. In this paper the same design model has been used to design a full information H_2 controller as described in [13, 14]. The performance specification weight has been adjusted during the developing phase so to optimize the controller performance, and it is shown in fig. 6. Results are also compared to those of a previous work on the H_2 control [14], in which only the blade root shear force was used as sensor and the baseline loads have not been filtered.

A summary of the hub loads reduction is shown in fig. 7. A first passive loads reduction, especially for the vertical force F_z, is obtained by replacing the Bo105 blades with the piezoelectric ones. The closed loop simulation with the output feedback controller shows a further reduction of vibratory loads. The 4/rev harmonic of the hub shear force F_Z is reduced by 43%, while the the hub moments M_X and M_Y benefits from a reduction of 65% and 58% respectively. Comparing the results with those obtained with the H_2 control, one can immediately notice that, in the case where only one sensor is used, the H_2 controller provides worst results especially if we observe the shear force

F_Z and the moment M_X. Using the same model and sensors, the dynamic compensator works better, with results that are comparable with those obtained by employing the direct output feedback strategy. In fact, while the static gain approach achieves a greater reduction of the vertical force F_Z, the H_2 control better alleviates M_Y. This is actually a good outcome for the applicability of the periodic output feedback controller, because with a simpler control law and a faster design it is possible to obtain good results while avoiding the implementation of a dynamic controller, which would involve a larger design space. It is also interesting to remark that harmonics higher than the $4/\mathrm{rev}$ are only marginally excited.

The applied control signal, for both the designed controllers, is shown in fig. 8. It is a sequence of steps because of the difference between the time steps of the simulation and the periodic controller. It is important to observe that the presented loads alleviation is obtained with reasonable control effort.

CONCLUSIONS

The hub vibratory loads of a Bo105 rotor model have been reduced by means of actively twisted blades, relying on periodic control theory. A periodic linearized model of the blade response is properly identified and a periodic direct output feedback controller which minimizes the $3/\mathrm{rev}$ and the $4/\mathrm{rev}$ harmonics of the blade root shear force has been designed. The controller performance are then compared to the ones of the dynamic compensator arising from the H_2 control theory. The closed loop simulations are performed through the coupling between MBDyn and Simulink.

The $4/\mathrm{rev}$ harmonic of the hub loads has been substantially reduced by the static controller for the given trim configuration and a major alleviation can be observed in the two moments M_X and M_Y. The macro-fiber composite piezoelectric actuator properties allow to maintain the control activity at low values.

A comparison with the H_2 controller, using the same design model, shows that the periodic static output feedback can be a valid substitute. In fact their performance are qute close, while the static control law involves very few parameters in the developing phase and the design algorithm is faster. Moreover, dealing with a static gain matrix suitable for all the sample times spanning the system period, a scheduling approach to cover the whole flight envelope of the helicopter is straightforward without all the complications that would arise when interpolating state space models [26, 27].

This application is based on a very simple aerodynamic theory. Further studies should be carried out to validate the designed controllers on a more accurate aerodynamic model able to reproduce the rotor wake and nonlinear effects, such as those due to transonic regime, dynamic stall and blade vortex interaction. More trim conditions should also be analyzed to prove the applicability of a gain scheduling algorithm while using output feedback controllers.

COPYRIGHT

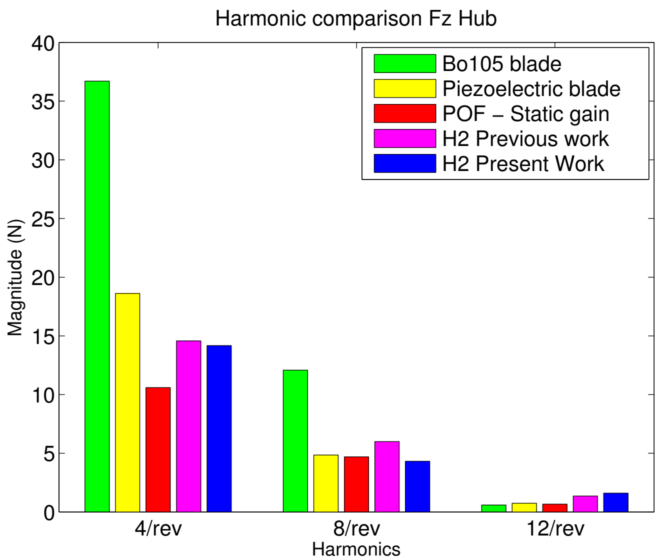

(a) Hub vertical force F_Z.

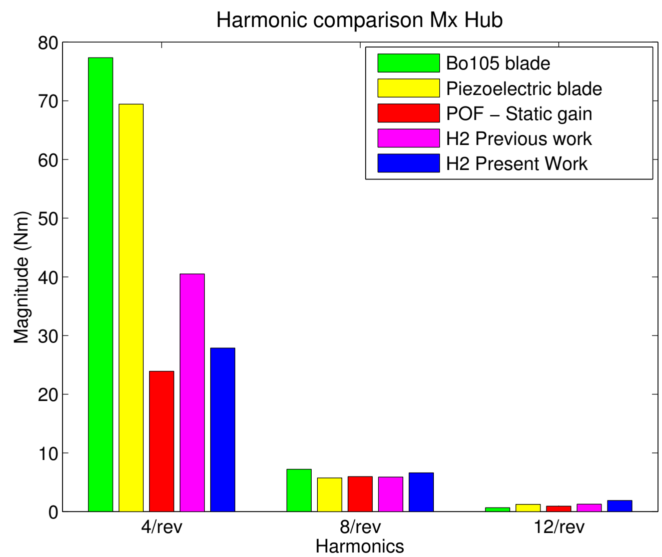

(b) Hub moment M_X.

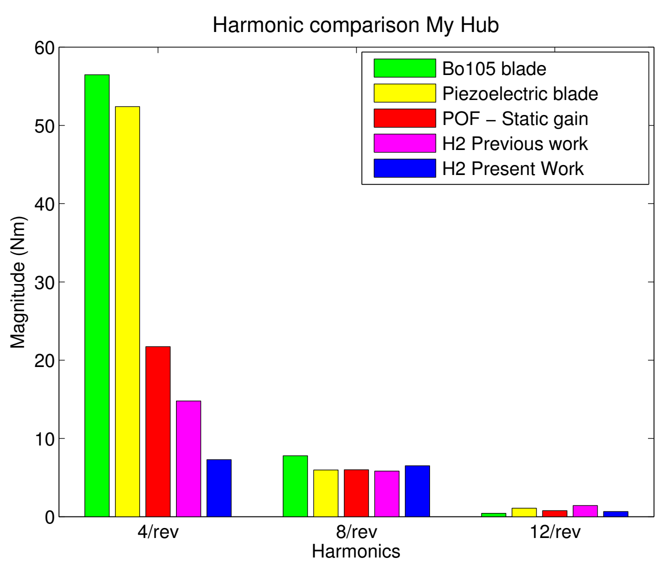

(c) Hub moment M_Y.

Figure 7: Vibrations reduction results.

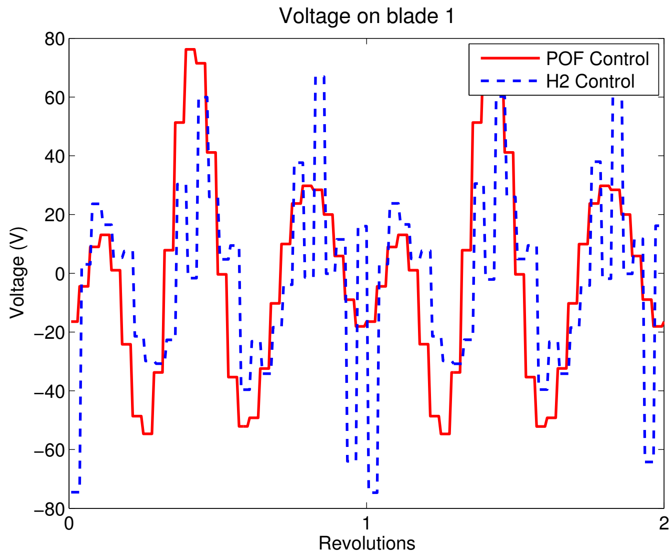

Figure 8: Blade 1 applied voltage.

APPENDIX

Solution of the discrete time periodic Lyapounov equations

This appendix details the algorithm for the solution of the DPLEs [23, 28].

Consider the reverse-time discrete periodic Lyapounov equation (RTDPLE) 13 and the forward-time discrete periodic Lyapounov equation (FTDPLE) 14. If the monodromy matrix $\Phi_A(N)$ of the dynamical system has no reciprocal eigenvalues, then it is possible to use a very simple solution method, based on reducing these problem to a single Lyapounov equation to compute a periodic generator. These equations can be solved by using standard methods. The rest of the solution is computed by backward- or forward-time recursion. This method is briefly described below for both equations.

- Solution of the RTDPLE: The periodic generator can be computed through the solution of the following discrete Lyapounov equation (DLE)

$$\mathbf{P}_1 = \Phi_A^T(N)\mathbf{P}_1\Phi_A(N) + \sum_{j=1}^{N} \Phi_A^T(j,1)\overline{\mathbf{Q}}_j\Phi_A(j,1),$$

  where $\Phi_A(j,i)$ is the transition matrix and the backward-time recursion is given by

$$\mathbf{P}_{N-i} = \overline{\mathbf{A}}_{N-i}^T\mathbf{P}_{N+1-i}\overline{\mathbf{A}}_{N-i} + \overline{\mathbf{Q}}_{N-i} \qquad i = 0,\ldots,N-2$$

- Solution of the FTDPLE: The periodic generator can be computed through the solution of the following DLE

$$\mathbf{S}_1 = \Phi_A(N)\mathbf{S}_1\Phi_A^T(N) + \sum_{j=1}^{N} \Phi_A(N+1, j+1)\mathbf{G}_j\Phi_A^T(N+1, j+1);$$

  the forward-time recursion is given by

$$\mathbf{S}_i = \overline{\mathbf{A}}_{i-1}\mathbf{S}_{i-1}\overline{\mathbf{A}}_{i-1}^T + \mathbf{G}_{i-1} \qquad i = 2, \ldots, N.$$

References

[1] D. Patt, J. Chandrasekar, D. S. Bernstein, and P. P. Friedmann. Higher-harmonic-control algorithm for helicopter vibration reduction revisited. *Journal of Guidance, Control and Dynamics*, 28(5), September-October 2005.

[2] Matthew L. Wilbur and W. Keats Wilkie. Active-twist rotor control applications for uavs. *24th US Army Science Conference*, 2004.

[3] A. Mander, D. Feszty, and F. Nitzsche. Active pitch link actuator for impedance control of helicopter vibration. *American Helicopter Society 64th Annual Forum*, 2008.

[4] Ashwani K. Padthe and Peretz P. Friedmann. Simultaneous bvi noise and vibration reduction in rotorcraft using microflaps including the effect of actuator saturation. *American Helicopter Society 68th Annual Forum*, 2012.

[5] K. Ravichandran, I. Chopra, Brian E. Wake, and B. Hein. Active pitch link actuator for impedance control of helicopter vibration. *American Helicopter Society 67th Annual Forum*, 2011.

[6] Hans Peter Monner, Johannes Riemenschneider, Steffen Opitz, and Martin Schulz. Development of active twist rotors at the german aerospace center (dlr). *American Institute of Aeronautics and Astronautics*, 2011.

[7] Johannes Riemenschneider and Steffen Opitz. Measurement of twist deflection in active twist rotor. *Aerospace Science and Technology*, 15:216–223, 2011.

[8] Prashant M Pawar and Sung Nam Jung. Active twist control methodology for vibration reduction of a hhelicopter with dissimilar rotor system. *Smart Materials and Structures*, 18, 2009.

[9] Matthias Althoff, Mayuresh J. Patil, and Johannes P. Traugott. Nonlinear modeling and control design of active helicopter blades. *Journal of the American Helicopter Society*, 57, 2012.

[10] R. Vaghi. *Studio Numerico del Controllo Ottimo di un Rotore Articolato di Elicottero con Applicazione alle Instabilitá di Flappeggio e Ritardo*. Master Thesis, Politecnico di Milano, Dipartimento di Ingegneria Aerospaziale, 1991.

[11] Paolo Arcara, Sergio Bittanti, and Marco Lovera. Periodic control of helicopter rotors for attenuation of vibrations in forward flight. *IEEE Transaction on Control Systems Technology*, 8(6), 2000.

[12] Sergio Bittanti and Francesco A. Cuzzola. Periodic active control of vibrations in helicopters: a gain-scheduled multi-objective approach. *Control Engineering Practice*, 10:1043–1057, 2002.

[13] Fatma Demet Ulker. *A New Framework For Helicopter Vibration Suppression; Time-Periodic System Identification and Controller Design*. PhD Thesis, Ottawa-Carleton Institute for Mechanical and Aerospace Engineering, April, 2011.

[14] Claudio Brillante, Marco Morandini, and Paolo Mantegazza. H2 periodic control on active twist rotor for vibration reduction. *AHS 70th Annual Forum and Technology Display, Montreal, Canada*, May 20-22, 2014.

[15] Oliver Dieterich, Joachim Götz, Binh DangVu, Henk Haverdings, Pierangelo Masarati, Marilena Pavel, Michael Jump, and Genaretti Massimiliano. Adverse rotorcraft-pilot coupling: Recent research activities in europe. *34th European Rotorcraft Forum (ERF)*, September 2008.

[16] P. Masarati, M. Morandini, and P. Mantegazza. An efficient formulation for general-purpose multibody/multiphysics analysis. *ASME J. Comput. Nonlinear Dyn.*, 2013.

[17] Gian Luca Ghiringhelli, Pierangelo Masarati, and Paolo Mantegazza. Multibody implementation of finite volume c0 beams. *AIAA Journal*, 38(1), 2000.

[18] G. L. Ghiringhelli, P. Masarati, and P. Mantegazza. Characterisation of anisotropic, non-homogeneous beam sections with embedded piezo-electric materials. *Journal of Intelligent Material Systems and Structures*, 8:842–858, 1997.

[19] Marco Morandini, Maria Chierichetti, and Paolo Mantegazza. Characteristic behavior of prismatic anisotropic beam via generalized eigenvectors. *International Journal of Solids and Structures*, 47:1327–1337, 2010.

[20] Marco Morandini Claudio Brillante and Paolo Mantegazza. Characterization of beam stiffness matrix with embedded piezoelectric devices via generalized eigenvectors. *International Journal of Solids and Structures*, 59:37–45, 2015.

[21] Gian Luca Ghiringhelli, Pierangelo Masarati, Marco Morandini, and Davide Muffo. Integrated aeroservoelastic analysis of induced strain rotor blades. *Mechanics of Advanced Materials and Structures*, 15:291–306, 2008.

[22] Michel Verhaegen and Xiaode Yu. A class of subspace model identification algorithms to identify periodically and arbitrarily time-varying systems. *Automatica*, 31:201–216, 1995.

[23] A. Varga and S. Pieters. A coputational approach for optimal periodic output feedback control. *IEEE International Symposium on Computer Aided Control System Design - CACSD*, 1996.

[24] Federico Fonte. *Active Gust Alleviation for a Regional Aircraft through Static Output Feedback*. Master Thesis, Politecnico di Milano, Departimento di Scienze e Tecnologie Aerospaziali, 2013.

[25] A. Varga. On solving periodic riccati equations. *Numerical Linear Algebra with Applications*, 2008.

[26] David Amsallem. Interpolation on manifolds of cfd-based fluid and finite element-based structural reduced-order models for on-line aeroelastic predictions. *PhD Thesis, Stanford University, Department of Aeronautics and Astronautics*, 2010.

[27] Jan De Caigny, Juan F. Camino, and Jan Swevers. Interpolation-based modeling of mimo lpv systems. *IEEE Transactions on Control Systems Technology*, 19(1), 2011.

[28] A. Varga. Periodic lyapounov equations: Some applications and new algorithms. *international Journal of Control*, 67:69–88, 1997.